Strongly deleterious mutations are a primary determinant of extinction risk due to inbreeding depression

Christopher C. Kyriazis[1*], Robert K. Wayne[1], Kirk E. Lohmueller[1,2,3*]

[1]Department of Ecology and Evolutionary Biology, University of California, Los Angeles
[2]Interdepartmental Program in Bioinformatics, University of California, Los Angeles
[3]Department of Human Genetics, David Geffen School of Medicine, University of California, Los Angeles
*Corresponding authors. Email: ckyriazis@g.ucla.edu; klohmueller@ucla.edu

Abstract

Human-driven habitat fragmentation and loss have led to a proliferation of small and isolated plant and animal populations with high risk of extinction. One of the main threats to extinction in these populations is inbreeding depression, which is primarily caused by the exposure of recessive deleterious mutations as homozygous by inbreeding. The typical approach for managing these populations is to maintain high genetic diversity, often by translocating individuals from large populations to initiate a 'genetic rescue.' However, the limitations of this approach have recently been highlighted by the demise of the gray wolf population on Isle Royale, which was driven to the brink of extinction soon after the arrival of a migrant from the large mainland wolf population. Here, we use a novel population genetic simulation framework to investigate the role of genetic diversity, deleterious variation, and demographic history in mediating extinction risk due to inbreeding depression in small populations. We show that, under realistic models of dominance, large populations harbor high levels of recessive strongly deleterious variation due to these mutations being hidden from selection in the heterozygous state. As a result, when large populations contract, they experience a substantially elevated risk of extinction after these strongly deleterious mutations are exposed by inbreeding. Moreover, we demonstrate that although translocating individuals to small populations is broadly effective as a means to reduce extinction risk, using small or moderate-sized source populations rather than large source populations can greatly increase the effectiveness of genetic rescue due to greater purging in these smaller populations. Our findings challenge the traditional conservation paradigm that focuses on maximizing genetic diversity to reduce extinction risk in favor of a view that emphasizes minimizing strongly deleterious variation. These insights have

important implications for managing small and isolated populations in the increasingly fragmented landscape of the Anthropocene.

Impact Summary

Numerous threats to extinction exist for small populations, including the detrimental effects of inbreeding. Although much of the focus in reducing these harmful effects in small populations has been on maintaining high genetic diversity, here we use simulations to demonstrate that emphasis should instead be placed on minimizing strongly deleterious variation. More specifically, we show that historically-large populations with high levels of genetic diversity also harbor elevated levels of recessive strongly deleterious mutations hidden in the heterozygous state. Thus, when these populations contract, inbreeding can expose these strongly deleterious mutations as homozygous and lead to severe inbreeding depression and rapid extinction. Moreover, we demonstrate that, although translocating individuals to these small populations to perform a 'genetic rescue' is broadly beneficial, the effectiveness of this strategy can be greatly increased by targeting historically-smaller source populations where recessive strongly deleterious mutations have been purged. These results challenge long-standing views on how to best conserve small and isolated populations facing the threat of inbreeding depression, and have immediate implications for preserving biodiversity in the increasingly fragmented landscape of the Anthropocene.

Introduction

The prevailing paradigm in conservation biology prioritizes the maintenance of high genetic diversity in small populations threatened with extinction due to inbreeding depression (Caughley 1994; Spielman et al. 2004). Under this paradigm, genetic diversity is considered one of the primary determinants of fitness (Allendorf and Leary 1986; Reed and Frankham 2003), and the harmful effects of inbreeding are thought to be minimized by maintaining genetic diversity. However, this thinking is challenged by the observation that some species, such as the Channel island fox, can persist at small population size with extremely low genetic diversity and show no signs of inbreeding depression (Robinson et al. 2016, 2018). This example and other similar studies suggest that, rather than being mediated by high genetic diversity, the persistence of small populations may instead be enabled by the purging of strongly deleterious mutations (Laws and Jamieson 2011; Xue et al. 2015; Hedrick and Garcia-Dorado 2016; Robinson et al. 2016, 2018; Van Der Valk et al. 2019; Grossen et al. 2020). In this study, we investigate how genetic diversity, deleterious variation, and demographic history influence extinction risk due to inbreeding depression using ecologically-realistic population genetic simulations. Our results demonstrate the central role of strongly deleterious variation in determining extinction risk due to inbreeding depression in small and isolated populations, and highlight the counterintuitive effects of strategies aimed at maintaining high genetic diversity. We argue that, in cases where populations are destined to remain small and isolated with high levels of inbreeding, management strategies should aim to minimize strongly deleterious variation rather than maximize genetic diversity.

The motivating example for our simulations is the gray wolf population on Isle Royale, an island in Lake Superior that has long served as a natural laboratory in ecology and conservation biology (Mech 1966; Peterson et al. 1984; Wayne et al. 1991; McLaren and Peterson 1994; Hedrick et al. 2019). Following 70 years of near-complete isolation at a size of ~10-50 individuals, the population was driven to the brink of extinction by severe inbreeding depression, with just two individuals remaining in 2018 (Hedrick et al. 2019; Robinson et al. 2019). Recent findings have suggested that the collapse of the population may have been

prompted by the introduction of high levels of recessive strongly deleterious variation by a migrant individual who arrived from the mainland in 1997 (Adams et al. 2011; Hedrick et al. 2014, 2019; Robinson et al. 2019). The high reproductive output of this individual on the island (34 offspring) led to intensive subsequent inbreeding in the population, driving these strongly deleterious mutations to high frequency and leading to severe inbreeding depression and ultimately the collapse of the population.

This example, although extreme, highlighted the potentially negative effects of founding or rescuing small populations with individuals from large and genetically-diverse populations. An alternative approach for genetic rescue or reintroduction initiatives could instead target historically-smaller populations where strongly deleterious mutations have been purged, or screen populations for individuals with low levels of strongly deleterious variation. The growing evidence for purging in wild populations (e.g., Xue et al. 2015; Robinson et al. 2018; Grossen et al. 2020) suggests that this approach may be effective as a means to decrease the severity of inbreeding depression in small populations at high risk of extinction. Given the ongoing reintroduction of wolves to Isle Royale, and the increasing necessity of reintroduction and genetic rescue more broadly (Whiteley et al. 2015; Frankham et al. 2017; Bell et al. 2019), such an approach could have wide-ranging implications for the conservation of small populations at risk.

The applicability of population genetic models to understanding extinction has historically been limited by unrealistic assumptions that often ignore stochastic ecological factors and rarely consider both weakly and strongly deleterious mutations (Lande 1994; Lynch et al. 1995; O'Grady et al. 2006; Caballero et al. 2017). Here, we use a novel population genetic simulation framework that combines realistic models of population dynamics with exome-scale genetic variation (Haller and Messer 2019) to assess how genetic diversity, deleterious variation, and demographic history influence extinction risk in small populations. Our simulations aim to capture the ecological factors that may contribute to extinction in small populations, such as those observed in the Isle Royale wolf population, by incorporating the effects of demographic

and environmental stochasticity, as well as natural catastrophes. Coupled with these stochastic population dynamics, we model a genome with parameters reflecting that of a canine exome, which accumulates neutral and deleterious mutations from an empirically-estimated distribution of fitness effects (Kim et al. 2017). Although our model is motivated by the Isle Royale wolf population, it is also intended to capture the dynamics of many other classic examples of population decline, inbreeding depression, and genetic rescue, such as Scandinavian wolves (Åkesson et al. 2016), Florida panthers (Johnson et al. 2010), and bighorn sheep (Hogg et al. 2006).

METHODS

Overview of the SLiM non-Wright-Fisher model

We conducted non-Wright-Fisher (nonWF) simulations using SLiM 3 (Haller and Messer 2019). The impetus for this model was to allow for more ecologically-realistic population genetic simulations by relaxing many of the restrictive assumptions of the Wright-Fisher model (Haller and Messer 2019). Such assumptions include non-overlapping generations and a fixed population size that is not influenced by fitness, both of which are unrealistic when trying to model the extinction of a population due to genetic factors.

Instead, the SLiM nonWF approach models population size (N) as an emergent property of individual absolute (rather than relative) fitness and a user-defined carrying capacity (K). Thus, if individual fitness declines, a population experiences extinction through a biologically realistic process (a fitness-driven reduction in population size). Further, the model includes overlapping generations, such that individuals with high fitness can survive and reproduce for multiple generations. At the start of each generation, each individual randomly mates with another individual in the population, with one offspring resulting from each mating. At the end of each generation, individuals die with a probability given by their absolute fitness (ranging from 0 to 1), which is rescaled by the ratio of K/N to model the effects of density dependence. Thus, the carrying capacity here does not directly determine the simulated population size, but rather it indirectly influences it through its impact on individual fitness and viability selection. For the

sake of both tractability and generality, we assume a hermaphroditic random mating population. A discussion of how the carrying capacity of a SLiM nonWF model is related to its Wright-Fisher effective population size is provided in the Supplementary Methods.

Demographic scenarios

To obtain a baseline understanding for how ancestral demography influences extinction risk in small populations, we first explored a 'population contraction' scenario with our simulations (Figure 1A). Here, we modeled an instantaneous contraction from a large 'ancestral population' ($K_{ancestral} \in \{1{,}000, 5{,}000, 10{,}000, 15{,}000\}$) to a small 'endangered population' ($K_{endangered} \in \{25, 50\}$) (Figure 1A). This contraction scenario could represent the isolation of a population with historical connectivity (e.g., the Florida panther population) or alternatively the founding of an isolated population through migration or translocation (e.g., the initial founding of the Isle Royale wolf population). For each contraction event, we randomly sampled $K_{endangered}$ number of individuals from the ancestral population to seed the endangered population after a burn in of $10*K_{ancestral}$ generations. All simulations were run until the endangered population went extinct. To examine the effects of a more gradual contraction, we also explored a scenario where an ancestral population with carrying capacity 10,000 first contracted to an intermediate carrying capacity of 1,000 for 200 generations, and finally an endangered carrying capacity of 25. We ran 25 simulation replicates for each combination of ancestral and endangered carrying capacities.

We next explored a 'genetic rescue' scenario, which similarly consisted of a population contraction from a large ancestral population to a small endangered population (Figure 1B). Here, however, we fixed the ancestral carrying capacity to 10,000, and again explored two endangered carrying capacities of 25 and 50. Prior to the contraction, we split off the following source populations for genetic rescue: 1) a large population remaining at the ancestral size (K=10,000); 2) a moderate-sized population with long-term isolation (K=1,000 for 1,000 generations); 3) a small population with relatively recent isolation (K=100 for 100 generations); and 4) a very small population with very recent isolation (K=25 for 10 generations). These

source population demographic histories were set to reflect a range of biologically-relevant scenarios (i.e., large and outbred populations, populations with moderate size and long-term isolation, smaller populations that have been more recently isolated) as well as provide a range of source population levels of genetic diversity and strongly deleterious variation to examine how these factors influence the efficacy of genetic rescue. Genetic rescue was initiated by translocating five randomly-selected individuals after the endangered population decreased in size to five or fewer individuals for the case when $K_{endangered}$=25 and 15 or fewer individuals for the case when $K_{endangered}$=50. Importantly, the exact number of generations of isolation for these source populations depended on the number of generations before translocation, which varied for each simulation replicate depending on the stochastic trajectory of the endangered population. For these simulations, we ran 50 replicates for simulations with $K_{endangered}$=25 and 25 replicates for simulations with $K_{endangered}$=50.

To further explore the dynamics of our genetic rescue scenario, we ran several additional simulations, here with endangered carrying capacity fixed to 25. First, to investigate the impact of selecting individuals for translocation to either maximize genetic diversity or minimize strongly deleterious variation, we ran simulations (50 replicates) were we picked selected five migrants from the K=10,000 source population with either the highest heterozygosity or fewest number of strongly deleterious alleles (where strongly deleterious mutations were defined to be those mutations with $s < -0.01$). We also explored scenarios with varying numbers of migrants (1, 5, or 10) with the number of translocations fixed to one, as well as varying the number of translocations (1, 2, or 5) with the number of migrants fixed to five. Here, we ran 25 replicates for each parameter combination. All simulations were run until the endangered population went extinct.

Stochastic population dynamics

To capture the non-genetic factors that can contribute to extinction in small populations (Caughley 1994), our model includes three sources of ecological stochasticity. First, demographic stochasticity was modelled using the built-in mechanics of the SLiM nonWF

model, in which survival from one generation to the next is determined by a Bernoulli trial with the probability of survival determined by the absolute fitness of an individual scaled by K/N (Haller and Messer 2019). Next, we incorporated the effects of environmental stochasticity in our simulations by modelling the carrying capacity of the endangered population as an Ornstein-Uhlenbeck process, in which the carrying capacity in a generation is given by:

$$\log(K(t+1)) = (1-\phi)K_{endangered} + \phi\log(K(t)) + w(0,\sigma)$$

where $\phi = 0.9$, $K_{endangered} \in \{25,50\}$ and $\sigma = \log_{10}(1.3)$ (Figure S1). The values of ϕ and σ were set arbitrarily to model environmental stochasticity with a moderate amount of variation and a high degree of auto-correlation. Finally, we modelled the effects of random natural catastrophes in our simulations by drawing a probability of mortality due to a catastrophe each generation from a beta distribution with $\alpha = 0.5$ and $\beta = 8$ (Figure S1). In each generation, deaths due to a catastrophe are then determined by the outcome of a Bernoulli trial for each individual with the probability given by the beta distribution. Environmental stochasticity and natural catastrophes were only modelled in the small endangered population. Importantly, these stochastic ecological effects rarely lead to extinction in the endangered population in the absence of deleterious variation (8/25 simulation replicates with neutral mutations extinct within 10,000 generations at $K_{endangered} = 25$, and none extinct for $K_{endangered} = 50$).

Genomic parameters

We set the genomic parameters in our simulations to model the exome of a wolf-like organism. To do this, each diploid individual in our simulation has 20,000 genes of length 1500 bp, which occur on 38 autosomes with the number of genes on each chromosome determined by the ratios observed in the dog genome (Lindblad-Toh et al. 2005). Recombination between these genes occurs at a rate of 1×10^{-3}, with no recombination within genes and free recombination between chromosomes. These genes accumulate neutral and deleterious mutations at a rate of 1×10^{-8} per site, with the ratio of deleterious to neutral mutations set to 2.31:1 (Huber et al. 2017; Kim et al. 2017). The selection coefficients for these deleterious mutations were drawn

230 from a distribution of fitness effects (DFE) estimated from a large sample of humans (Kim et al.
231 2017; see Supplementary Methods for additional details).
232
233 We initially set the dominance coefficients for our simulations according to a *hs* relationship
234 inferred for yeast (Agrawal and Whitlock 2011) following the approach from Henn et al. 2016
235 with the following functional form:

236 $$h(s) = \frac{1/2}{(1+7071.07 \times s)}$$

237 This *hs* relationship intends to capture the pattern evident in empirical data that the dominance
238 coefficient of a mutation tends to be inversely related to its selection coefficient, such that the
239 most strongly deleterious mutations are highly recessive (Simmons and Crow 1977; Agrawal
240 and Whitlock 2011; Huber et al. 2018). However, we found that simulations with this *hs*
241 relationship in SLiM were extremely computationally intensive (see Supplementary Methods),
242 such that we were only able to obtain results for simulations with the smallest ancestral
243 carrying capacities of 1,000 and 5,000.
244
245 To overcome these computational limitations for realistic models of dominance, we instead
246 implemented an approach assuming that weakly/moderately deleterious mutations ($s \geq -0.01$)
247 were partially recessive (h=0.25) and strongly deleterious mutations ($s < -0.01$) were fully
248 recessive (h=0). The aim of this approach (hereafter referred to as our "*hmix*" model) was to
249 capture the key feature of the *hs* relationship that more deleterious mutations tend to be more
250 recessive, with the dominance coefficients for these two classes of mutations reflecting their
251 mean dominance coefficient under the *hs* relationship (Figure S2). Given our finding that the
252 behavior of this model is extremely similar to that of the *hs* relationship (see Results), we use
253 the *hmix* model for all simulations except where otherwise noted. More details on how the
254 *hmix* model was implemented in SLiM is provided in the Supplementary Methods.
255
256 To further explore the impact of dominance coefficients, we also ran simulations where we
257 varied the dominance coefficient for all mutations ($h \in \{0, 0.01, 0.05, 0.2, 0.5\}$). In addition, we
258 explored the impact of decreasing the number of sites in which fully recessive (h=0) deleterious

259 mutations can occur (i.e. the mutational target size) by varying the number of genes in our
260 simulations ($g \in$ {1,000, 5,000, 10,000, 15,000, 20,000}). These simulations were run solely
261 under the 'population contraction' demographic scenario with $K_{ancestral} \in$ {1,000, 5,000, 10,000,
262 15,000} and $K_{endangered}$ = 25. We ran 25 replicates for each of these simulations, terminating the
263 simulation when the endangered population went extinct.
264
265 During the simulations, we kept track of several summaries of the state of the population.
266 These include the population's mean heterozygosity, mean inbreeding coefficient (F_{ROH}), the
267 mean fitness, and the average number of deleterious alleles per individual binned into weakly (-
268 $0.001 < s \leq -0.00001$), moderately ($-0.01 < s \leq -0.001$), strongly ($s < -0.01$), and very strongly ($s <$
269 -0.05) deleterious classes. Fitness was calculated multiplicatively across sites. Here, we
270 restricted F_{ROH} to include only runs of homozygosity greater than 1 Mb to capture inbreeding
271 due to mating between close relatives. These statistics were calculated from a sample of 30
272 individuals every 1000 generations during the burn-in and every generation following the
273 contraction.
274
275 *Burn-in conditions for the simulations*
276 Our simulations during the burn-in retained fixed mutations and did not model reverse
277 mutation. Retaining fixed mutations during the burn-in was important to ensure that weakly
278 deleterious mutations that drifted to fixation contribute to absolute fitness. However, one
279 consequence of retaining fixed mutations is that there is no mutation-selection-drift
280 equilibrium in the ancestral population since weakly deleterious mutations continue to
281 accumulate as fixations even after heterozygosity of segregating variation has leveled off
282 (Figure S3). As a result, fitness during the burn-in also never reaches equilibrium, but instead
283 declines gradually as weakly deleterious mutations are fixed. Although fixation of weakly
284 deleterious mutations occurs at a rate that is inverse to population size (i.e., much faster in
285 smaller populations), we found that this effect is cancelled out when the length of the burn-in is
286 proportional to the population's carrying capacity (i.e., 10*K, leading to a much shorter burn-in
287 for smaller populations), resulting in the same pre-contraction fitness regardless of population

size (Figure S4a). To explore the effect of reducing the pre-contraction fitness of the smaller populations, we ran simulations under a fully recessive model (*h*=0) where we added an additional 20,000 generations to the burn-in for the K=1,000, K=5,000, and K=10,000 populations, leading to burn-in durations of 30,000, 70,000, and 120,000 respectively (10*K + 20,000). This led to a notable reduction in pre-contraction fitness for the K=1,000 population and more moderate reductions in fitness for the larger populations (Figure S4). However, there was no differences in time to extinction (Figure S4C), suggesting that extinction dynamics are governed more by the numbers of recessive strongly deleterious alleles in these populations rather than their pre-bottleneck fitness. This finding is further supported by our simulation results that demonstrate that strongly deleterious mutations are a far more important determinant of extinction times compared to weakly or moderately deleterious mutations (see Results). Thus, for the sake of computational tractability, we ran all burn-ins for $10*K_{ancestral}$ generations.

Results

Population contraction simulations under *hmix* model

Our population contraction simulations demonstrate that, although larger populations have higher genetic diversity (Figure 2A), they also harbor higher levels of strongly deleterious variation (Figure 2B). Consequently, we observe a strong effect of ancestral demography on time to extinction following a population contraction, with populations that were historically large experiencing more rapid extinction (Figure 2C). For example, given an endangered carrying capacity of 25, a population with an ancestral carrying capacity of 1,000 will go extinct in 474 generations on average, whereas a population with an ancestral carrying capacity of 15,000 will do so in 70 generations on average (Figure 2C). When modelling a more gradual contraction from an ancestral carrying capacity of 10,000, we found that extinction times were slightly increased relative to the instantaneous contraction scenario (Figure S5), suggesting that more gradual contractions can facilitate purging and ultimately decrease extinction risk.

316 Examination of individual simulation replicates provides insight into the dynamics of extinction
317 in these populations (Figures 3A and S6). Endangered populations with an ancestral carrying
318 capacity of 1,000 contain fewer strongly deleterious mutations, translating to a decreased
319 severity of inbreeding depression and ultimately longer persistence (Figures 3A and S6). This
320 decreased severity of inbreeding depression allows these populations to become highly inbred
321 ($F_{ROH} \approx 1$) well before going extinct (Figures 3A and S6). By contrast, endangered populations
322 with a larger ancestral carrying capacity of 15,000 have much higher levels of recessive strongly
323 deleterious variation due to these mutations being hidden from selection in the ancestral
324 population, resulting in a more rapid loss of fitness as these populations become inbred
325 (Figures 3B and S6). As a result, these populations typically go extinct well before F_{ROH}
326 approaches one (Figures 3B and S6). These populations also lose fitness due to increased
327 genetic drift and inbreeding among more distant relatives, which is not captured by our
328 definition of F_{ROH}.
329
330 Following contraction, the ability of the endangered population to purge its load of recessive
331 deleterious mutations also depended on stochastic ecological factors. For example, when the
332 carrying capacity of the endangered population was, by chance, higher due to environmental
333 stochasticity, natural selection was most effective at removing strongly deleterious alleles,
334 translating to longer persistence (Figures 3 and S6). By contrast, when the carrying capacity of
335 the endangered population was low soon after contraction, purging tended to be less effective,
336 resulting in more rapid extinction (Figures 3 and S6). However, in both cases, purging was also
337 counteracted by continual input of strongly deleterious alleles by mutation, which eventually
338 contributed to population extinction. Overall, these various sources of genetic and ecological
339 stochasticity together resulted in highly variable extinction times for any given parameter
340 settings, highlighting the important role of random events in determining whether a small
341 population can persist.
342
343 Our simulations also demonstrate the importance of increasing the carrying capacity of the
344 endangered population as a means to ensure population persistence. Larger endangered

345 populations (K=50) were better able to purge recessive deleterious mutations following the
346 contraction, resulting in much longer persistence (Figure S7). Moreover, larger populations
347 were less impacted by stochastic ecological factors, which also contributed to increased time to
348 extinction. Nevertheless, extinction times for these larger endangered populations still
349 depended strongly on the ancestral carrying capacity (Figure S7), demonstrating the
350 importance of considering both recent and historical demography when assessing extinction
351 risk.
352
353 **Results under varying genomic parameters**
354 We next explored the sensitivity of our results to the genomic parameters assumed in our
355 model. In particular, we focus on the impact of dominance coefficients, as previous work has
356 suggested that the extent to which strongly deleterious mutations accumulate at higher
357 frequencies in larger populations depends strongly on the assumed dominance coefficients (Nei
358 1968; Hedrick 2002; Hedrick and Garcia-Dorado 2016). Under the most realistic model of an *hs*
359 relationship, we found that strongly deleterious mutations do accumulate at much higher
360 frequencies in larger populations, leading to much faster extinction following contraction
361 (Figure 4). However, we also found that simulations with an *hs* relationship in SLiM were
362 extremely computationally intensive, such that we were unable to obtain results for the larger
363 ancestral carrying capacities of 10,000 and 15,000 (see Supplementary Methods). Nevertheless,
364 these results demonstrate a strong concordance between the *hs* relationship and our *hmix*
365 model, suggesting that our *hmix* model captures the key features of the *hs* relationship (Figures
366 4 and S2).
367
368 When assuming a single dominance coefficient for all mutations, our results demonstrate a
369 range of outcomes that depended on the assumed dominance coefficient. Specifically, when
370 assuming h=0 or 0.01, we again find that larger populations harbor higher levels of strongly
371 deleterious variation, with strikingly similar patterns to the *hs* relationship or *hmix* model
372 (Figure 4). However, this effect is greatly diminished when mutations are only partially
373 recessive (h=0.05 or 0.2), and is nonexistent when mutations are additive (h=0.5), as expected

374 (Figure 4). Notably, although the average dominance coefficient under our assumed *hs*
375 relationship is approximately 0.2 (Agrawal and Whitlock 2011), our results with h=0.2 are
376 dramatically different from those under the *hs* relationship (Figure 4).
377
378 To further investigate the importance of strongly vs weakly/moderately deleterious mutations
379 in our *hmix* model, we ran simulations where we truncated our DFE to only permit strongly
380 deleterious ($s < -0.01$ and h=0) or weakly/moderately deleterious mutations ($s \geq -0.01$ and
381 h=0.25) to enter the population. More specifically, in the case of permitting only strongly
382 deleterious mutations, we allowed any mutation with $s < -0.01$ to enter the population as
383 normal, however mutations with $s \geq -0.01$ instead became neutral mutations. Here, our results
384 for simulations that only included strongly deleterious mutations were notably similar to the
385 full *hmix* model, with extinction times that depended strongly on ancestral demography (Figure
386 S8). By contrast, results for simulations that only included weakly/moderately deleterious
387 mutations were dramatically different from the full model, and had greatly increased extinction
388 times (Figure S8). Given that strongly deleterious mutations constitute only ~25% of all new
389 deleterious mutations under our assumed DFE (Kim et al. 2017), these results strikingly
390 demonstrate their disproportionate impact on extinction risk relative to the effects of more
391 weakly or moderately deleterious mutations.
392
393 As a final way of exploring the impact of recessive deleterious mutations, we also conducted
394 simulations where we decreased the target size for deleterious mutations assuming h=0. The
395 motivation for these simulations was to test whether we would still observe an impact of
396 ancestral demography on extinction times when lowering the number of genes that could
397 accumulate fully recessive deleterious mutations. To do this, we decreased the number of
398 genes (g) in our simulations from 20,000 to $g \in$ {1,000, 5,000, 10,000, and 15,000}. Here, we
399 observed that the effect of ancestral demography is still present, though greatly diminished,
400 with as few as 1,000 genes, and remains substantial with as few as 5,000 genes (Figure S9).
401
402 **Genetic rescue simulations**

403 We next explored how demography and strongly deleterious variation impact the effectiveness
404 of genetic rescue assuming an *hmix* model of dominance. Here, we quantify the effectiveness of
405 genetic rescue as the extent to which the introduction of migrants to the endangered
406 population increased extinction times. When translocating five migrants from one of four
407 source populations (Figure 5A-B) to an endangered population with K=25, we found that all
408 source populations led to increases in time to extinction relative to a no-rescue scenario (Figure
409 5C). Importantly, however, we found that the magnitude of increase in time to extinction was
410 highly dependent on source population demography and levels of strongly deleterious
411 variation. For example, whereas genetic rescue from the large source population (K=10,000) led
412 to a notable increase in mean time to extinction of 16%, rescue from the moderate-sized source
413 population resulted in a much more dramatic increase of 130% (Figure 5C). Genetic rescue from
414 small and moderately-inbred populations (Figure S10) also resulted in increases in mean time to
415 extinction that were at least as great as that of the large source population (63% increase for
416 K=100, 13% increase for K=25) (Figure 5C). We observed similar patterns when conducting
417 simulations with a larger endangered population (K=50) (Figure S11), though the beneficial
418 effects of genetic rescue were somewhat diminished, likely due to the larger recipient
419 population size when translocation was initiated (N ≤ 15) as well as the greater efficacy of
420 purging within the larger recipient population.
421
422 Examination of individual replicates again offers insight into the factors driving extinction in
423 these populations (Figures 6 and S12). In all simulated scenarios, we observed a large increase
424 in fitness immediately following the introduction of migrants (Figures 6 and S12), likely due to
425 the high strength of heterosis (masking of fixed recessive deleterious alleles) following initial
426 admixture. In most cases, these increases in fitness led to population growth, though the extent
427 to which population sizes increased was strongly influenced by environmental stochasticity
428 (Figures 6 and S12). Soon after genetic rescue, however, the resumption of inbreeding again led
429 to a decline in fitness (Figures 6 and S12). Here, the rate of fitness decline was determined by
430 the levels of strongly deleterious variation in the migrant individuals and their descendants. For
431 example, when translocation occurred from a large source population (K=10,000), levels of

strongly deleterious variation remained high after genetic rescue, eventually resulting in severe inbreeding depression once inbreeding resumed (Figure 6). By contrast, when the moderate-sized source population was used (K=1,000), levels of strongly deleterious variation dramatically decreased following genetic rescue, greatly decreasing the severity of inbreeding depression in future generations (Figure 6).

These results demonstrate that, although the larger source populations have higher fitness and genetic diversity, they also harbor a high number of heterozygous recessive strongly deleterious mutations (Figures 5 and S10). These mutations are quickly made homozygous by inbreeding in the endangered population following translocation, exacerbating the severity of inbreeding depression and eventually contributing to extinction. In support of this interpretation, we found that time to extinction following genetic rescue is predicted by the average number of strongly deleterious alleles per individual in the source population when examining all source populations simultaneously (Figure 5D). By contrast, we found that average source population heterozygosity was not very predictive of time to extinction, where in fact we observed a slight negative correlation due to the fact that source populations with higher genetic diversity also tend to harbor higher levels of recessive strongly deleterious variation (Figure 5E). We obtained similar results when restricting this analysis to the K=25 source population, the source population for which there was the highest variability in strongly deleterious variation and genetic diversity (Figure S13). However, in this case, we do see strong negative correlation between genetic diversity and extinction times, which is likely driven by heterozygosity being correlated with strongly deleterious variation at this intra-population scale.

Our finding that source population strongly deleterious variation predicts the efficacy of genetic rescue suggests that genome-wide levels of deleterious variation could be used to select individuals for genetic rescue. We explored the efficacy of this strategy by selecting the individuals with the fewest strongly deleterious alleles ($s < -0.01$) from the large source population (K=10,000) for rescue. This approach resulted in an increase in mean time to extinction of 74% compared to the non-rescue scenario, a 49% increase relative to randomly

461 selecting individuals from the large source population (Figure 5F). By contrast, when individuals
462 with the highest genome-wide heterozygosity were selected, we observed an increase in time
463 to extinction that was no greater than when individuals were selected at random (Figure 5F).
464 These results further support the causal relationship between strongly deleterious variation
465 and extinction risk due to inbreeding depression, as well as the lack of this relationship
466 between heterozygosity and extinction risk.
467
468 Lastly, we explored the effects of varying the number of migrants (1, 5, or 10) as well as the
469 number of translocation events (1, 2, or 5), focusing on the K=10,000 and K=1,000 source
470 populations. These simulations show persistent increases in time to extinction with increasing
471 number of translocations regardless of the source population (Figure S14), suggesting that the
472 efficacy of genetic rescue does not diminish with each additional migration event. When
473 varying the number of migrants, we found that extinction times increased slightly in the case
474 where migrants were drawn from the K=1,000 source population, but did not increase when
475 drawing migrants from the K=10,000 source population (Figure S14).
476
477 **Discussion**
478 Our simulations demonstrate the central importance of demographic history and recessive
479 strongly deleterious mutations in determining the risk of extinction due to inbreeding
480 depression in small and isolated populations. We find that populations that were historically
481 large have a much higher risk of extinction following a population contraction compared to
482 historically-smaller populations (Figure 2). These findings may be counterintuitive given the
483 thinking that small populations should be less fit due to an accumulation of weakly deleterious
484 alleles (Kimura et al. 1963; Lynch and Gabriel 1990; Lynch et al. 1995; Battaillon and Kirkpatrick
485 2000). The key insight that our simulations highlight is that larger ancestral populations harbor
486 more recessive strongly deleterious mutations (Figure 2), due to these mutations being hidden
487 from purifying selection as heterozygotes. The exposure of these mutations as homozygous by
488 inbreeding in small populations can lead to dramatic reductions in fitness and drive rapid
489 extinction, well before 'mutational meltdown' due to an accumulation of weakly deleterious

490 mutations can occur (Lynch and Gabriel 1990; Lynch et al. 1995). By demonstrating that this
491 effect is sufficient to ultimately drive extinction on short timescales, our simulations illustrate
492 the importance of recessive deleterious variation as a mechanism of inbreeding depression
493 (Charlesworth and Willis 2009; Hedrick and Garcia-Dorado 2016). Notably, we do not include
494 any forms of heterozygote advantage in our model, which represents an alternative mechanism
495 for inbreeding depression, though one that has received far less empirical support
496 (Charlesworth and Willis 2009; Hedrick and Garcia-Dorado 2016). Thus, our finding that
497 recessive deleterious mutations alone can drive rapid extinction in small populations serves as
498 further support for these mutations being the primary cause of inbreeding depression.
499
500 Although the insight that strongly deleterious mutations that are fully recessive can accumulate
501 at greater frequencies in larger populations has been noted elsewhere (Nei 1968; Hedrick 2002;
502 Hedrick and Garcia-Dorado 2016; Szpiech et al. 2019), our results add to this work by
503 demonstrating that that these effects persist under realistic genomic parameters and models of
504 dominance, including both an *hs* relationship and our *hmix* model (Figure 4). This result is due
505 to the fact that strongly deleterious mutations under these models tend to be highly recessive
506 (Simmons and Crow 1977; Agrawal and Whitlock 2011; Huber et al. 2018), and are therefore
507 hidden from purifying selection when present as heterozygotes in large populations Moreover,
508 when examining models with a single dominance coefficient for all mutations, we find that our
509 results with fully recessive mutations (h=0 or 0.01) are highly similar to those under more
510 realistic models of dominance, whereas the impact of ancestral demography is greatly
511 diminished with partially recessive (h=0.05 or 0.2) mutations and nonexistent with additive
512 (h=0.5) mutations (Figure 4). Given that the mean dominance coefficient under our assumed *hs*
513 relationship is 0.2 (Agrawal and Whitlock 2011), the strong dissimilarity between our results
514 under an *hs* relationship and when assuming h=0.2 for all mutations is notable, and suggests
515 that the key factor mediating extinction dynamics is the presence of fully recessive strongly
516 deleterious mutations, rather than the overall mean dominance coefficient. In support of this
517 interpretation, we show that simulations that only include the fraction of mutations that are
518 strongly deleterious and fully recessive (h=0) exhibit extinction times that are highly similar to

extinction times under an *hs* relationship or *hmix* model, whereas simulations that only include the fraction of mutations that are weakly or moderately deleterious and partially recessive (*h*=0.25) have much longer extinction times that depend only minimally on ancestral demography (Figure S8). This result is especially striking when considering that strongly deleterious mutations comprise only ~25% of the overall number of deleterious mutations under our assumed DFE (Kim et al. 2017). Taken together, these results further bolster our conclusion that strongly deleterious mutations are the primary determinant of extinction risk due to inbreeding depression in small populations. However, gaining a more precise understanding of these dynamics will greatly depend on improving our knowledge of the distribution of dominance coefficients across various taxa.

The considerable influence of ancestral demography on extinction risk that our simulations reveal has important implications for assessing the threat of extinction due to inbreeding depression in wild populations. Quantifying inbreeding depression in the wild and predicting the threat it poses to extinction remains a major challenge in conservation biology, and the reasons why some small populations suffer from inbreeding depression and others do not is often unclear (Hedrick and Garcia-Dorado 2016). Our simulations demonstrate that these differences may be determined in large part by the ancestral demography of a species. Consequently, we suggest that information on ancestral demography, which is increasingly becoming accessible using genomic data (Beichman et al. 2018), should be more widely incorporated into extinction risk predictions. In particular, given that nearly all threatened populations have recently undergone reductions in size due to anthropogenic pressures, these results suggest that their continued persistence may depend crucially on their ancestral demography and load of recessive strongly deleterious mutations. In addition, our results also suggest that island populations that have historically been small may in fact have reduced extinction risk due to genetic factors due to their high isolation and smaller population size, which may have facilitated purging of recessive strongly deleterious mutations (Laws and Jamieson 2011; Robinson et al. 2018). However, our simulations also reveal that the fate of small populations is highly stochastic, and that even under the same ecological and genetic

548 parameters, time to extinction can vary substantially (Figures 2 and 4). Thus, predictions of
549 extinction risk for any wild population should necessarily be accompanied by a fair amount of
550 uncertainty.
551
552 Our results also provide insight on how best to conduct a genetic rescue, which is becoming
553 increasingly necessary for maintaining small and isolated populations under growing
554 anthropogenic pressures (Whiteley et al. 2015; Hedrick and Garcia-Dorado 2016; Frankham et
555 al. 2017; Bell et al. 2019). Consistent with many other studies (e.g., Hogg et al. 2006; Johnson et
556 al. 2010; Frankham 2015; Åkesson et al. 2016), our simulations highlight the beneficial effects
557 of genetic rescue, supporting recent calls for its more widespread application (Whiteley et al.
558 2015; Frankham et al. 2017; Bell et al. 2019). However, in stark contrast to existing
559 recommendations (Pickup et al. 2012; Whiteley et al. 2015), we found that targeting large
560 source populations with high genetic diversity was among the least effective genetic rescue
561 strategies (Figures 5 and S11). Instead, our results demonstrate that the effectiveness of
562 genetic rescue can potentially be maximized by drawing migrants from moderate-sized source
563 populations which have fewer strongly deleterious mutations (Figures 5 and S11). These source
564 populations are ideal due to being small enough to carry few strongly deleterious recessive
565 mutations in the heterozygous state, but not so small that they accumulate a substantial load of
566 fixed weakly or moderately deleterious mutations. Finally, our results demonstrate that even
567 small and somewhat inbred populations can also serve as effective source populations (Figures
568 5C and S10), as other studies have shown (Heber et al. 2012b,a).
569
570 Although our results suggest that large populations may not be ideal source populations for
571 genetic rescue, we demonstrate that the effectiveness of this strategy can be greatly increased
572 when individuals are screened for low levels of strongly deleterious variation (Figure 5F).
573 However, applications of such approach may remain limited by our ability to accurately predict
574 the fitness consequences of individual mutations, which remains a major challenge even in
575 humans (Eilbeck et al. 2017). Our results also demonstrate that repeated genetic rescue from
576 large or moderate-sized source populations can result in persistent beneficial effects (Figure

577 S14), highlighting the efficacy of this strategy for populations that are destined to remain small
578 and isolated. One inevitable consequence of this or any other genetic rescue strategy, however,
579 is a loss of native ancestry (Johnson et al. 2010; Adams et al. 2011; Harris et al. 2019), which can
580 potentially swamp out locally adapted alleles (though see Fitzpatrick et al. 2020). Although we
581 do not track levels of admixture in our simulations, it is probable that the post-rescue
582 populations are composed of highly admixed individuals (Harris et al. 2019).
583
584 In addition to providing guidelines for how to best conduct a genetic rescue, our results also
585 have implications for understanding the mechanisms underlying genetic rescue. Two
586 mechanisms have generally been proposed for genetic rescue: heterosis (masking of fixed
587 recessive deleterious mutations) and adaptive evolution (increases in fitness due to selection
588 on new alleles) (Whiteley et al. 2015). By demonstrating that, even in the absence of adaptive
589 variation, migration into small and inbred populations can lead to increases in fitness and
590 demographic rates consistent with those observed in empirical systems (e.g., Hogg et al. 2006;
591 Johnson et al. 2010; Adams et al. 2011; Åkesson et al. 2016), our results suggest that heterosis
592 alone may be able to explain much of the beneficial effects of genetic rescue. However, a more
593 thorough investigation of the relative roles of heterosis and adaptive evolution as mechanisms
594 of genetic rescue could be conducted by incorporating adaptive mutations into our simulation
595 framework. Finally, our finding that increases in fitness following migration do not always lead
596 to increases in population size due to the effects of environmental stochasticity (Figure S12)
597 suggests that definitions of genetic rescue based on demographic effects alone may be
598 restrictively narrow, as other authors have suggested (Hedrick et al. 2011). In particular, this
599 result has relevance to the debate of whether the Isle Royale wolf population truly experienced
600 a genetic rescue, given that the population size did not increase substantially following
601 migration, perhaps due to poor environmental conditions (Adams et al. 2011; Hedrick et al.
602 2011)
603
604 Our simulation framework has several notable limitations. First, due to the high computational
605 load of our simulations (see Supplementary Methods), we were unable to examine ancestral

606 populations with carrying capacities larger than 15,000, limiting the observed impact of
607 ancestral demography. Second, we did not examine heterozygote advantage as a potential
608 mechanism for inbreeding depression, which could impact the negative relationship between
609 extinction times and source population heterozygosity that we observed (Figure 5E). However,
610 empirical support for heterozygote advantage as a mechanism for inbreeding depression is
611 scarce (Charlesworth and Willis 2009; Hedrick and Garcia-Dorado 2016), suggesting that it may
612 not substantially impact our results. In addition, we did not include adaptive mutations in our
613 model, which may also be relevant to the ability of small populations to persist under
614 environmental change, as well as for exploring the impacts of outbreeding depression due to
615 differential local adaptation. Although recent work has suggested that concerns about
616 outbreeding depression may have been overstated (Whiteley et al. 2015; Frankham et al.
617 2017), assessing its influence in determining source population selection nevertheless
618 represents an important area for future research. Finally, we emphasize that the demographic
619 scenarios explored here may not be applicable to all small and isolated populations. Specifically,
620 our assumption of an instantaneous contraction from a large ancestral population to a small
621 endangered population may not capture the demographic trajectory of many populations that
622 have experienced more gradual declines. In these cases, a gradual decline may have facilitated
623 purging of strongly deleterious mutations (Figure S5), decreasing the necessity for genetic
624 rescue (e.g., Xue et al. 2015; Robinson et al. 2018). Overall, we recommend that any
625 conservation actions motivated by our results carefully consider the demography of the
626 population of interest, ideally using simulations.
627
628 In conclusion, our results highlight the detrimental effects of strongly deleterious variation in
629 small populations, and suggest that many conservation strategies for endangered species may
630 be improved by minimizing strongly deleterious variation rather than maximizing
631 heterozygosity. These results are especially relevant to the ongoing reintroduction of wolves to
632 Isle Royale, which has been guided by the goal of maximizing the genetic diversity of the new
633 population. Although our simulations are motivated by this example, by examining a wide
634 range of demographic scenarios, our results have implications beyond the Isle Royale wolf

population. Future research should explore implementation of these strategies by expanding the use of genomic tools and assessments of deleterious variation in the context of the conserving small and isolated populations (Fitzpatrick and Funk 2019). Given the great expense of most translocation programs, incorporating genomic approaches represents a sound investment with the potential to substantially postpone the need for future intervention.

Acknowledgements

We are grateful to Jacqueline Robinson, Bernard Kim, Brad Shaffer, Marty Kardos, and members of the Lohmueller and Wayne labs for helpful feedback and ideas. We thank Ben Haller for assistance with SLiM. This research was supported by NIH grant R35GM119856 (to K.E.L.).

Author Contributions

CCK and KEL conceived the project, CCK ran the simulations and analyzed the results, all authors contributed to writing and editing the manuscript.

Data Accessibility

Simulation and data processing scripts are available at https://github.com/ckyriazis/genetic_rescue_simulations.

References

Adams, J. R., L. M. Vucetich, P. W. Hedrick, R. O. Peterson, and J. A. Vucetich. 2011. Genomic sweep and potential genetic rescue during limiting environmental conditions in an isolated wolf population. Proc. R. Soc. B Biol. Sci. 278:3336–3344.

Agrawal, A. F., and M. C. Whitlock. 2011. Inferences about the distribution of dominance drawn from yeast gene knockout data. Genetics 187:553–566.

Åkesson, M., O. Liberg, H. Sand, P. Wabakken, S. Bensch, and Ø. Flagstad. 2016. Genetic rescue in a severely inbred wolf population. Mol. Ecol. 25:4745–4756.

Allendorf, F. W., and R. F. Leary. 1986. Heterozygosity and fitness in natural populations of animals. Pp. 58–72 *in* Conservation biology: the science of scarcity and diversity.

Battaillon, T., and M. Kirkpatrick. 2000. Inbreeding depression due to mildly deleterious mutations in finite populations: size does matter. Genet. Res. (Camb). 75:75–81.

Beichman, A. C., E. Huerta-Sanchez, and K. E. Lohmueller. 2018. Using Genomic Data to Infer Historic Population Dynamics. Annu. Rev. Ecol. Evol. Syst. 49:433–456.

Bell, D. A., Z. L. Robinson, W. C. Funk, S. W. Fitzpatrick, F. W. Allendorf, D. A. Tallmon, and A. R. Whiteley. 2019. The Exciting Potential and Remaining Uncertainties of Genetic Rescue. Trends Ecol. Evol. 1–11. Elsevier Ltd.

Caballero, A., I. Bravo, and J. Wang. 2017. Inbreeding load and purging: Implications for the short-term survival and the conservation management of small populations. Heredity (Edinb). 118:177–185. Nature Publishing Group.

Caughley, G. 1994. Directions in Conservation Biology. J. Anim. Ecol. 63:215–244.

Charlesworth, D., and J. H. Willis. 2009. The genetics of inbreeding depression. Nat. Rev. Genet. 10:783–796.

Eilbeck, K., A. Quinlan, and M. Yandell. 2017. Settling the score: Variant prioritization and Mendelian disease. Nat. Rev. Genet. 18:599–612. Nature Publishing Group.

Fitzpatrick, S. W., G. S. Bradburd, C. T. Kremer, P. E. Salerno, L. M. Angeloni, and W. C. Funk. 2020. Genomic and Fitness Consequences of Genetic Rescue in Wild Populations. Curr. Biol. 30:1–6. Elsevier Ltd.

Fitzpatrick, S. W., and W. C. Funk. 2019. Genomics for Genetic Rescue. P. *in* Wildlife Conservation Genomics.

Frankham, R. 2015. Genetic rescue of small inbred populations: meta-analysis reveals large and consistent benefits of gene flow. Mol. Ecol. 24:2610–2618.

Frankham, R., J. D. Ballou, K. Ralls, M. Eldridge, M. R. Dudash, C. B. Fenster, R. C. Lacy, and P. Sunnucks. 2017. Genetic Management of Fragmented Animal and Plant Populations. Oxford University Press, Oxford, UK.

Grossen, C., F. Guillaume, L. F. Keller, and D. Croll. 2020. Purging of highly deleterious mutations through severe bottlenecks in Alpine ibex. Nat. Commun. 11:1001. Springer US.

Haller, B. C., and P. W. Messer. 2019. SLiM 3: Forward Genetic Simulations Beyond the Wright-Fisher Model. Mol. Biol. Evol. 36:632–637.

Harris, K., Y. Zhang, and R. Nielsen. 2019. Genetic rescue and the maintenance of native ancestry. Conserv. Genet. 20:59–64. Springer Netherlands.

Heber, S., J. V. Briskie, and L. A. Apiolaza. 2012a. A test of the “genetic rescue” technique using bottlenecked donor populations of Drosophila melanogaster. PLoS One 7.

Heber, S., A. Varsani, S. Kuhn, A. Girg, B. Kempenaers, and J. Briskie. 2012b. The genetic rescue

of two bottlenecked South Island robin populations using translocations of inbred donors. Proc. R. Soc. B Biol. Sci. 280.
Hedrick, P. W. 2002. Lethals in Finite Populations. Evolution (N. Y). 56:654–657.
Hedrick, P. W., J. R. Adams, and J. A. Vucetich. 2011. Reevaluating and Broadening the Definition of Genetic Rescue. Conserv. Biol. 25:1069–1070.
Hedrick, P. W., and A. Garcia-Dorado. 2016. Understanding Inbreeding Depression, Purging, and Genetic Rescue. Trends Ecol. Evol. 31:940–952. Elsevier Ltd.
Hedrick, P. W., R. O. Peterson, L. M. Vucetich, J. R. Adams, and J. A. Vucetich. 2014. Genetic rescue in Isle Royale wolves: genetic analysis and the collapse of the population. Conserv. Genet. 15:1111–1121.
Hedrick, P. W., J. A. Robinson, R. O. Peterson, and J. A. Vucetich. 2019. Genetics and extinction and the example of Isle Royale wolves. Anim. Conserv. 22:302–309.
Henn, B. M., L. R. Botigué, S. Peischl, I. Dupanloup, M. Lipatov, B. K. Maples, A. R. Martin, S. Musharoff, H. Cann, M. P. Snyder, L. Excoffier, J. M. Kidd, and C. D. Bustamante. 2016. Distance from sub-Saharan Africa predicts mutational load in diverse human genomes. Proc. Natl. Acad. Sci. 113:E440–E449.
Hogg, J. T., S. H. Forbes, B. M. Steele, and G. Luikart. 2006. Genetic rescue of an insular population of large mammals. Proc. R. Soc. B 273:1491–1499.
Huber, C. D., A. Durvasula, and A. M. Hancock. 2018. Gene expression drives the evolution of dominance. Nat. Commun. 9:1–11. Springer US.
Huber, C. D., B. Y. Kim, C. D. Marsden, and K. E. Lohmueller. 2017. Determining the factors driving selective effects of new nonsynonymous mutations. Proc. Natl. Acad. Sci. 114:4465–4470.
Johnson, W. E., D. P. Onorato, M. E. Roelke, E. D. Land, M. Cunningham, R. C. Belden, R. McBride, D. Jansen, M. Lotz, D. Shindle, J. G. Howard, D. E. Wildt, L. M. Penfold, J. A. Hostetler, M. K. Oli, and S. J. O'Brien. 2010. Genetic restoration of the Florida panther. Science (80-.). 329:1641–1645.
Kim, B. Y., C. D. Huber, and K. E. Lohmueller. 2017. Inference of the Distribution of Selection Coefficients for New Nonsynonymous Mutations Using Large Samples. Genetics 206:345–361.
Kimura, M., T. Maruyama, and J. F. Crow. 1963. The mutation load in small populations. Genetics 1303–1312.
Lande, R. 1994. Risk of population extinction from fixation of new deleterious mutations. Evolution (N. Y). 48:1460–1469.
Laws, R. J., and I. G. Jamieson. 2011. Is lack of evidence of inbreeding depression in a threatened New Zealand robin indicative of reduced genetic load? Anim. Conserv. 14:47–55.
Lindblad-Toh, K., C. M. Wade, T. S. Mikkelsen, E. K. Karlsson, D. B. Jaffe, M. Kamal, M. Clamp, J. L. Chang, E. J. Kulbokas, M. C. Zody, E. Mauceli, X. Xie, M. Breen, R. K. Wayne, E. A. Ostrander, C. P. Ponting, F. Galibert, D. R. Smith, P. J. DeJong, E. Kirkness, P. Alvarez, T. Biagi, W. Brockman, J. Butler, C. W. Chin, A. Cook, J. Cuff, M. J. Daly, D. DeCaprio, S. Gnerre, M. Grabherr, M. Kellis, M. Kleber, C. Bardeleben, L. Goodstadt, A. Heger, C. Hitte, L. Kim, K. P. Koepfli, H. G. Parker, J. P. Pollinger, S. M. J. Searle, N. B. Sutter, R. Thomas, C. Webber, and E. S. Lander. 2005. Genome sequence, comparative analysis and haplotype

743 structure of the domestic dog. Nature 438:803–819.
744 Lynch, M., I. J. Conery, and R. Burger. 1995. Mutation accumulation and the extinction of small
745 populations. Am. Nat. 146:489–518.
746 Lynch, M., and W. Gabriel. 1990. Mutation load and the survival of small populations. Evolution
747 (N. Y). 44:1725–1737.
748 McLaren, B. E., and R. O. Peterson. 1994. Wolves, Moose, and Tree Rings on Isle Royale. Science
749 (80-.). 266:1555–1558.
750 Mech, L. D. 1966. The Wolves of Isle Royale.
751 Nei, M. 1968. The frequency distribution of lethal chromosomes in finite populations. Proc.
752 Natl. Acad. Sci. 60:517–524.
753 O'Grady, J. J., B. W. Brook, D. H. Reed, J. D. Ballou, D. W. Tonkyn, and R. Frankham. 2006.
754 Realistic levels of inbreeding depression strongly affect extinction risk in wild populations.
755 Biol. Conserv. 133:42–51.
756 Peterson, R. O., R. E. Page, and K. M. Dodge. 1984. Wolves, Moose, and the Allometry of
757 Population Cycles. Science (80-.). 224:1350–1352.
758 Pickup, M., D. L. Field, D. M. Rowell, and A. G. Young. 2012. Source population characteristics
759 affect heterosis following genetic rescue of fragmented plant populations. Proc. R. Soc. B
760 280:1–9.
761 Reed, D. H., and R. Frankham. 2003. Correlation between Fitness and Genetic Diversity.
762 Conserv. Biol. 17:230–237.
763 Robinson, J. A., C. Brown, B. Y. Kim, K. E. Lohmueller, and R. K. Wayne. 2018. Purging of Strongly
764 Deleterious Mutations Explains Long-Term Persistence and Absence of Inbreeding
765 Depression in Island Foxes. Curr. Biol. 28:1–8. Elsevier Ltd.
766 Robinson, J. A., D. Ortega-Del Vecchyo, Z. Fan, B. Y. Kim, B. M. Vonholdt, C. D. Marsden, K. E.
767 Lohmueller, and R. K. Wayne. 2016. Genomic Flatlining in the Endangered Island Fox. Curr.
768 Biol. 26:1183–1189. Elsevier Ltd.
769 Robinson, J. A., J. Räikkönen, L. M. Vucetich, J. A. Vucetich, R. O. Peterson, K. E. Lohmueller, and
770 R. K. Wayne. 2019. Genomic signatures of extensive inbreeding in Isle Royale wolves, a
771 population on the threshold of extinction. Sci. Adv. 5:1–13.
772 Simmons, M. J., and J. F. Crow. 1977. Mutations affecting fitness in Drosophila populations.
773 Ann. Rev. Genet. 11:49–78.
774 Spielman, D., B. W. Brook, and R. Frankham. 2004. Most species are not driven to extinction
775 before genetic factors impact them. Proc. Natl. Acad. Sci. 101:15261–15264.
776 Szpiech, Z. A., A. C. Mak, M. J. White, D. Hu, C. Eng, E. G. Burchard, and R. D. Hernandez. 2019.
777 Ancestry-dependent Enrichment of Deleterious Homozygotes in Runs of Homozygosity.
778 Am. J. Hum. Genet. 105:1–16. ElsevierCompany.
779 Van Der Valk, T., M. De Manuel, T. Marquez-Bonet, and K. Guschanski. 2019. Estimates of
780 genetic load suggest extensive genetic purging in mammalian populations. bioRxiv.
781 Wayne, R., N. Lehman, D. Girman, P. Gogan, D. Gilbert, K. Hansen, R. Peterson, U. Seal, A.
782 Eisenhawer, L. Mech, and R. J. Krumenaker. 1991. Conservation Genetics of the
783 Endangered Isle Royale Gray Wolf. Conserv. Biol. 5:41–51.
784 Whiteley, A. R., S. W. Fitzpatrick, W. C. Funk, and D. A. Tallmon. 2015. Genetic rescue to the
785 rescue. Trends Ecol. Evol. 30:42–49. Elsevier Ltd.
786 Xue, Y., J. Prado-Martinez, P. H. Sudmant, V. Narasimhan, Q. Ayub, M. Szpak, P. Frandsen, Y.

Chen, B. Yngvadottir, D. N. Cooper, M. De Manuel, J. Hernandez-rodriguez, I. Lobon, H. R. Siegismund, L. Pagani, M. A. Quail, C. Hvilsom, A. Mudakikwa, E. E. Eichler, M. R. Cranfield, and T. Marques-bonet. 2015. Mountain gorilla genomes reveal the impact of long-term population decline and inbreeding. Science (80-.). 348:242–245.

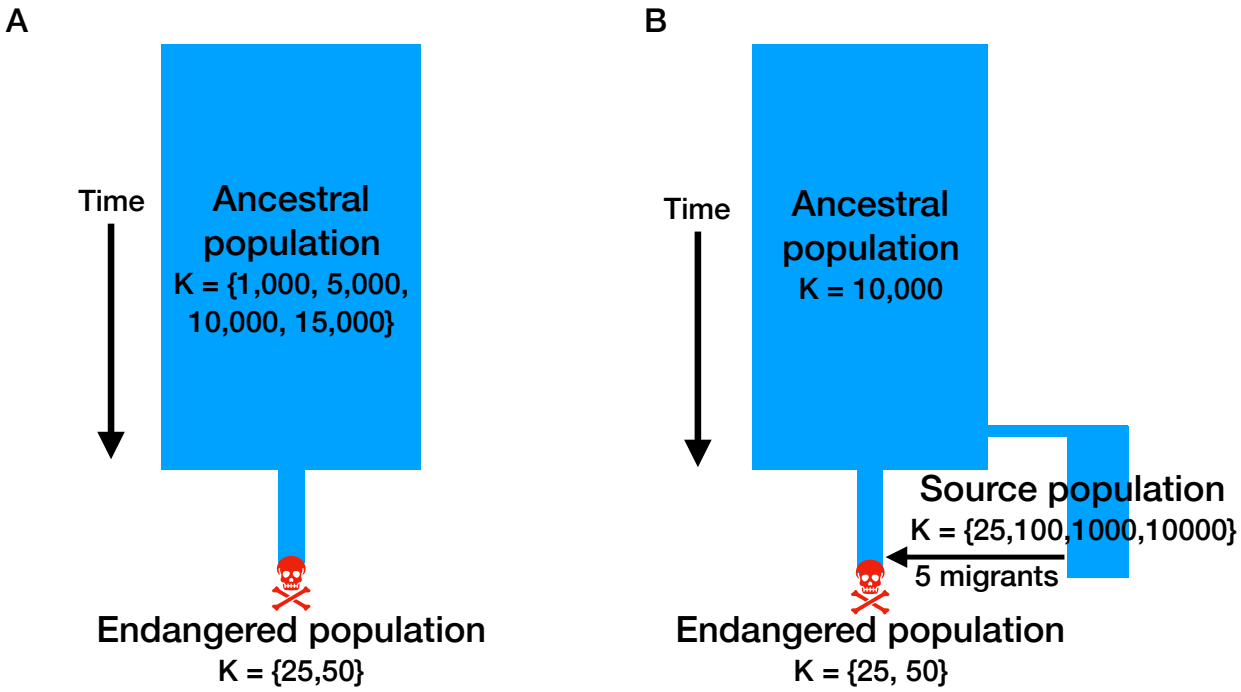

Figure 1: Schematic of the demographic scenarios used for simulations. (A) Schematic for 'population contraction' simulations. (B) Schematic for 'genetic rescue' simulations. Note that migration occurs in the genetic rescue scenario when the endangered population decreases in size to five or fewer individuals when $K_{endangered}$ =25 and 15 or fewer individuals when $K_{endangered}$ =50.

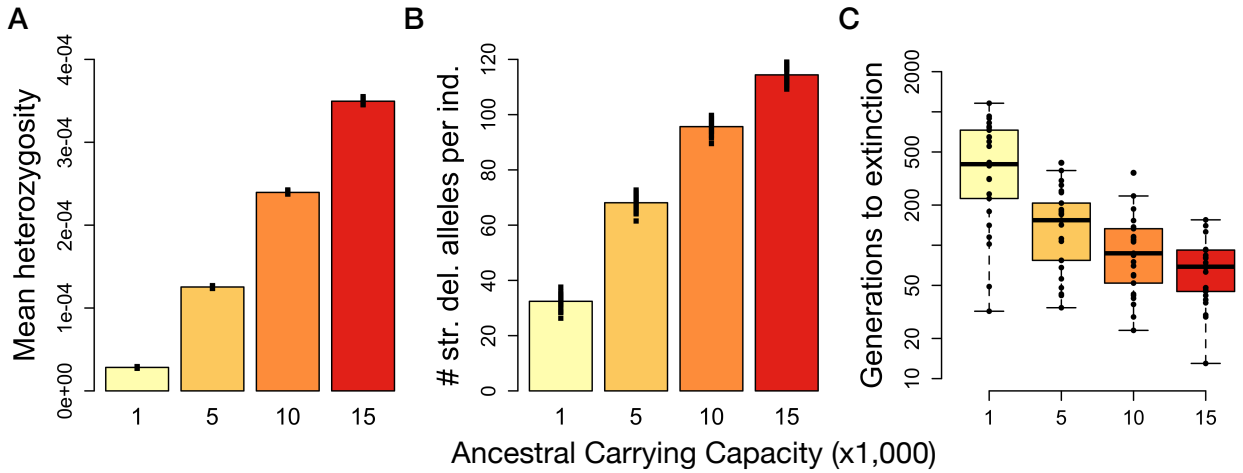

Figure 2: Results for population contraction simulations under the *hmix* model of dominance. (A) Mean heterozygosity of ancestral populations prior to contraction. (B) Average number of strongly deleterious alleles ($s < -0.01$) per individual in the ancestral populations prior to contraction. (C) Time to extinction following contraction from ancestral populations of varying size to an endangered population with K=25. Extinction times for $K_{endangered} = 50$ shown in Figure S8. Note that the y-axis is on a log scale. For each parameter setting, 25 simulation replicates were run.

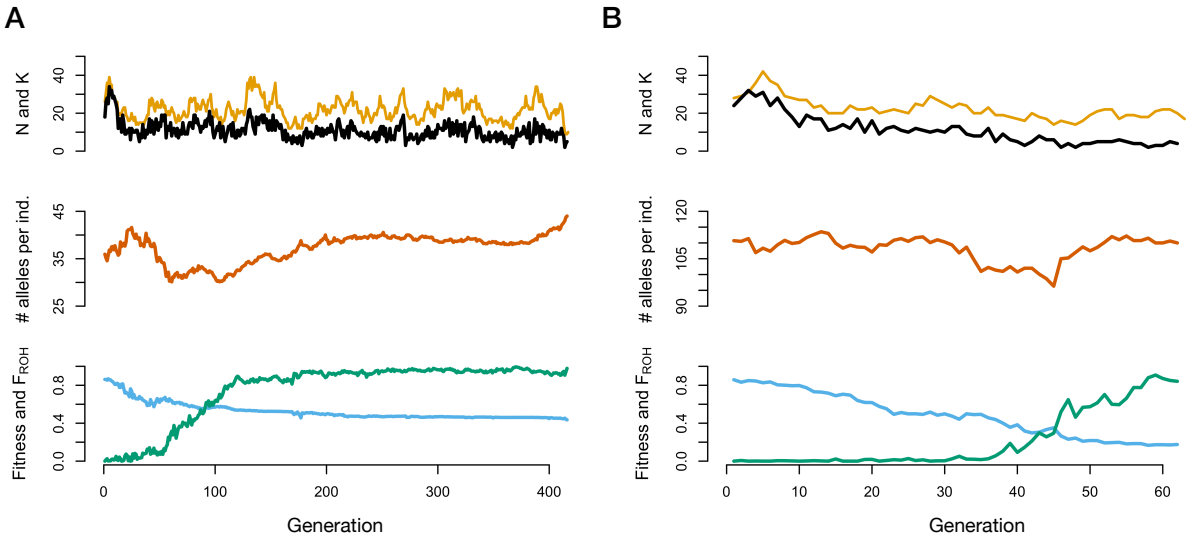

Figure 3: Representative examples of population contraction simulations with ancestral populations of varying size. (A) Example with $K_{ancestral}$ = 1,000. (B) Example with $K_{ancestral}$ = 15,000. The top of each panel shows population size (N) in black and carrying capacity (K) in gold, the middle shows the average number of strongly deleterious alleles (s < -0.01) per individual, and the bottom shows mean absolute fitness in blue and mean inbreeding coefficient (F_{ROH}) in green. For both replicates, $K_{endangered}$ = 25 and an *hmix* model of dominance was assumed. Note the differing y-axis scales for the middle panels and differing x-axis scales for panels A and B.

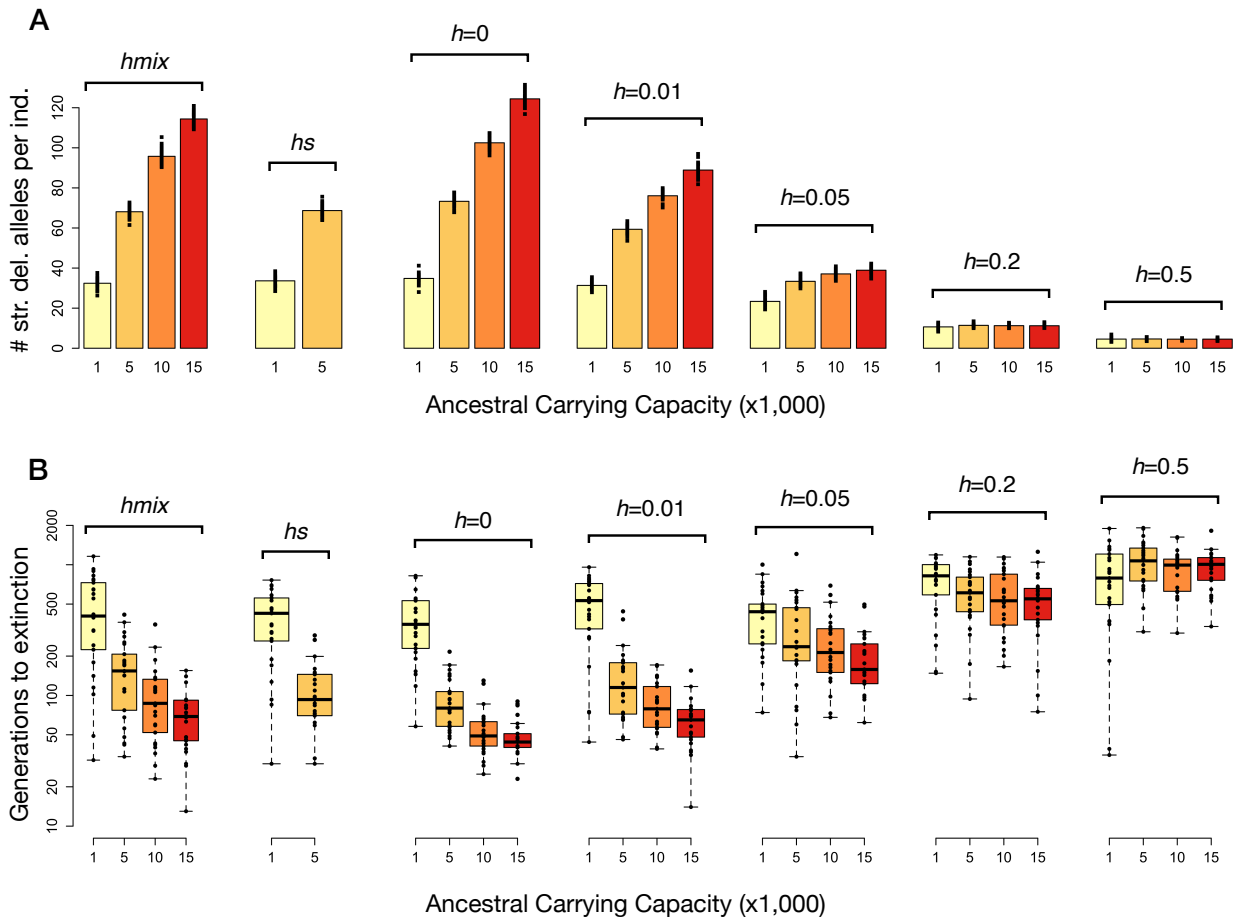

Figure 4: Impact of dominance coefficients on the accumulation of strongly deleterious mutations and extinction times following a contraction. (A) Mean number of strongly deleterious alleles per individual (s < -0.01) prior to contraction in ancestral populations of varying size and under varying models of dominance. (B) Time to extinction following contraction to $K_{endangered}$ = 25 plotted on a log scale. Note that we were unable to obtain results for $K_{ancestral}$ = 10,000 and 15,000 under the *hs* relationship due to computational limitations. For each parameter setting, 25 simulation replicates were run.

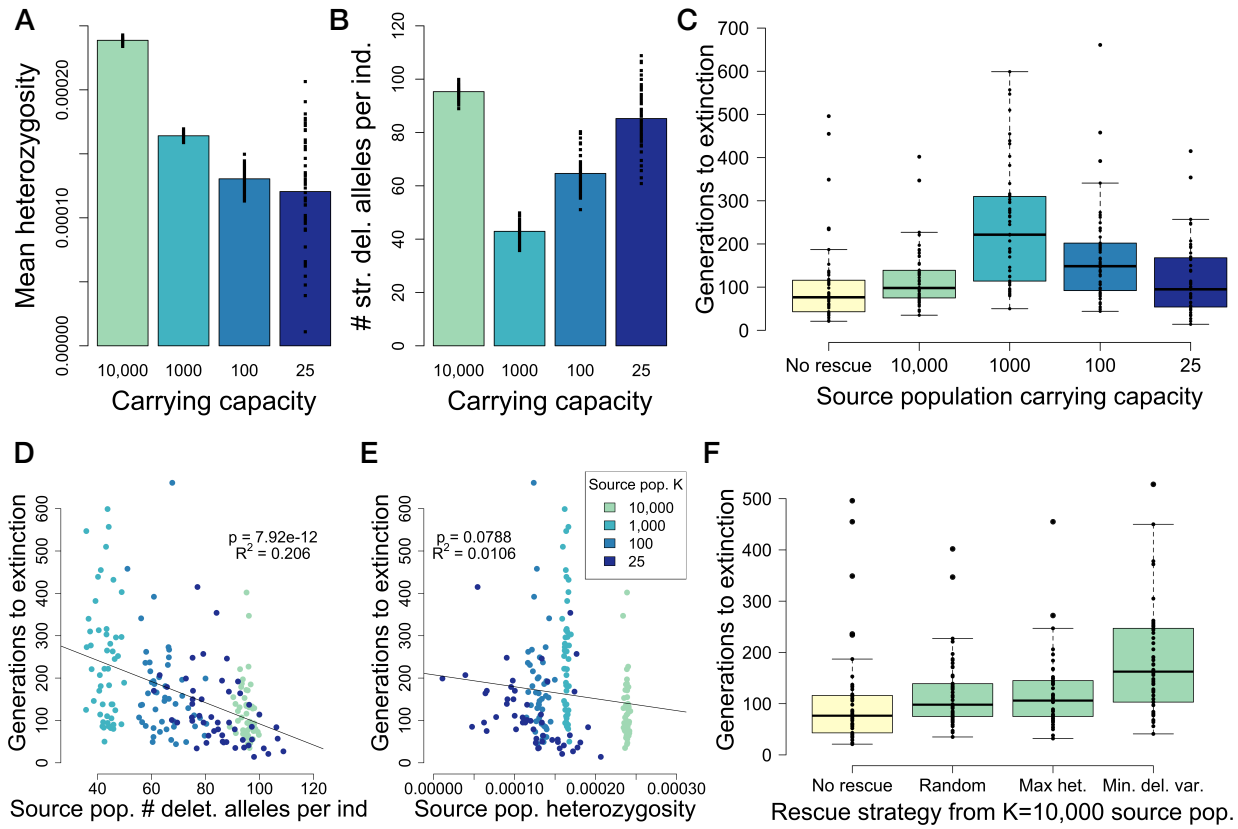

Figure 5: Source population deleterious variation determines the effectiveness of genetic rescue. (A) Average heterozygosity of source populations used for genetic rescue during the generation of rescue. (B) Mean number of strongly deleterious alleles ($s < -0.01$) per individual in the source populations used for genetic rescue. See Figure S10 for source population fitness and levels of inbreeding. (C) Time to extinction following genetic rescue from source populations of varying size. (D) Time to extinction following genetic rescue is negatively correlated with the number of recessive strongly deleterious alleles ($s < -0.01$) per individual used for rescue. (E) Time to extinction following genetic rescue is not correlated with the heterozygosity of the source population. See Figure S13 for regression results when considering only the K=25 source population. (F) Time to extinction under different strategies of genetic rescue from the K=10,000 source population. For each parameter setting, 50 simulation replicates were run.

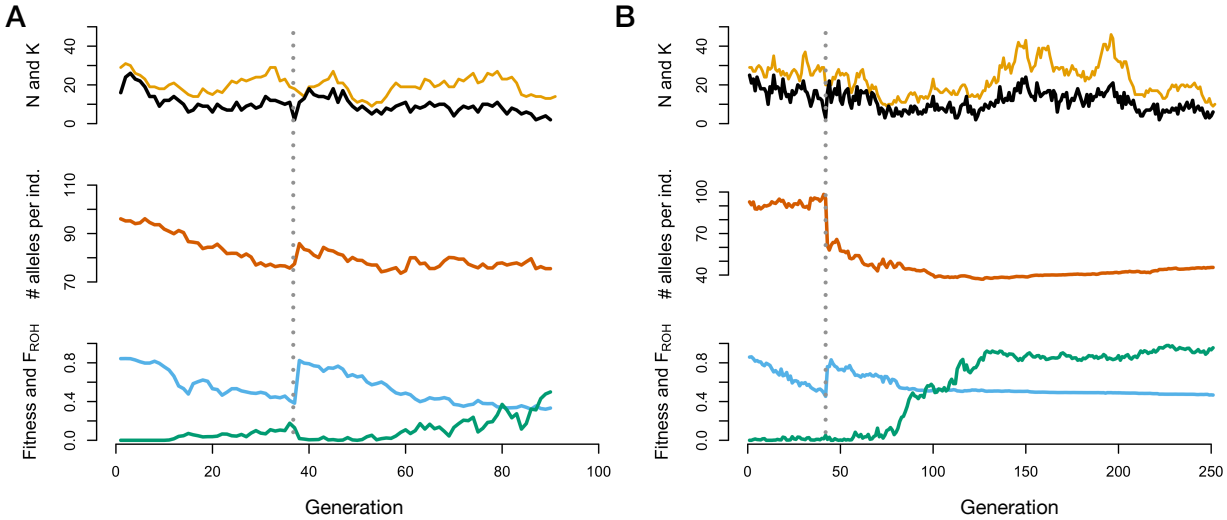

Figure 6: Representative examples of genetic rescue simulations with source populations of varying size. (A) Example when a large source population (K=10,000) is used for genetic rescue. (B) Example when a moderate-sized (K=1,000) is used. The top of each panel shows population size (N) in black and carrying capacity (K) in gold, the middle shows the average number of strongly deleterious alleles (*s* < -0.01) per individual, and the bottom shows mean absolute fitness in blue and mean inbreeding coefficient (F_{ROH}) in green. The dashed grey line indicates the generation in which migration occurred. For both replicates, $K_{endangered}$ = 25 and an *hmix* model of dominance was assumed. Note the differing y-axis scales for the middle panels and differing x-axis scales for panels A and B.